

SAND REPORT

SAND2006-1739
Unlimited Release
Printed April 2006

Aluminum Equation of State Validation and Verification for the ALEGRA HEDP Simulation Code

Kyle Cochrane, Mike Desjarlais, Tom Haill,
Jeff Lawrence, Marcus Knudson and Greg Dunham

Prepared by
Sandia National Laboratories
Albuquerque, New Mexico 87185 and Livermore, California 94550

Sandia is a multiprogram laboratory operated by Sandia Corporation,
a Lockheed Martin Company, for the United States Department of Energy's
National Nuclear Security Administration under Contract DE-AC04-94-AL85000.

Approved for public release; further dissemination unlimited.



Sandia National Laboratories

Issued by Sandia National Laboratories, operated for the United States Department of Energy by Sandia Corporation.

NOTICE: This report was prepared as an account of work sponsored by an agency of the United States Government. Neither the United States Government, nor any agency thereof, nor any of their employees, nor any of their contractors, subcontractors, or their employees, make any warranty, express or implied, or assume any legal liability or responsibility for the accuracy, completeness, or usefulness of any information, apparatus, product, or process disclosed, or represent that its use would not infringe privately owned rights. Reference herein to any specific commercial product, process, or service by trade name, trademark, manufacturer, or otherwise, does not necessarily constitute or imply its endorsement, recommendation, or favoring by the United States Government, any agency thereof, or any of their contractors or subcontractors. The views and opinions expressed herein do not necessarily state or reflect those of the United States Government, any agency thereof, or any of their contractors.

Printed in the United States of America. This report has been reproduced directly from the best available copy.

Available to DOE and DOE contractors from
U.S. Department of Energy
Office of Scientific and Technical Information
P.O. Box 62
Oak Ridge, TN 37831

Telephone: (865) 576-8401
Facsimile: (865) 576-5728
E-Mail: reports@adonis.osti.gov
Online ordering: <http://www.doe.gov/bridge>

Available to the public from
U.S. Department of Commerce
National Technical Information Service
5285 Port Royal Rd
Springfield, VA 22161

Telephone: (800) 553-6847
Facsimile: (703) 605-6900
E-Mail: orders@ntis.fedworld.gov
Online ordering: <http://www.ntis.gov/help/ordermethods.asp?loc=7-4-0#online>



SAND2006-1739
Unlimited Release
Printed April 2006

Aluminum Equation of State Validation and Verification for the ALEGRA HEDP Simulation Code

Kyle Cochrane, Mike Desjarlais, Tom Hail, and Jeff Lawrence
HEDP Theory and ICF Target Design

Marcus Knudson
Shock and Z-Pinch Physics

Greg Dunham
Diagnostics and Target Physics

Sandia National Laboratories
P.O. Box 5800
Albuquerque, NM 87185-1186

Abstract

Determining whether an equation of state (EOS) table is valid for a given regime requires several steps that include confirming that it obeys the thermodynamic consistency relations and that the table matches available existing experimental data. Once the EOS is analyzed, then we must ensure the simulation code can reproduce analytical results.

In this report, we show analytical results of Hugoniot calculations and compare them with values calculated from experimental $U_s - U_p$ data. Next we check that the tables are thermodynamically consistent. Then, we show analytical results of impedance matching using one of the aluminum EOS models and compare those analytical results to data. Finally, ALEGRA-HEDP is used to run a pseudo 1-D shock simulation, which is compared to the analytical model with an error of approximately 0.1%. This implies that ALEGRA-HEDP can simulate the shock Hugoniot to within the error of the EOS table when compared to the experimental data for an ideal simulation.

Acknowledgment

We would like to thank Tim Trucano for his many helpful comments and insight, Chris Garasi for his direction, and Tom Mehlhorn for the opportunity to pursue interesting topics.

Contents

1	Introduction	9
2	Calculating Hugoniot	9
3	Thermodynamic Consistency	11
4	Impedance Matching	12
5	ALEGRA-HEDP Simulation	13
6	Comparing ALEGRA-HEDP with Experimental Data	14
7	Conclusion	14
	References	27

List of Figures

1	Hugoniot points for 6 EOS tables and experimental data.	15
2	Aluminum 3720 EOS Tables.	16
3	Error in thermodynamic consistency for aluminum Table 3720.	17
4	Error in thermodynamic consistency for aluminum Table 3719.	18
5	Error in thermodynamic consistency for aluminum QEOS.	19
6	Consistency error in isentropic release simulations.	20
7	Impedance matching on a $P - U_p$ plot.	21
8	Time slice from the end of an ALEGRA-HEDP simulation.	22
9	Shock position vs. time.	23
10	Impedance matching on a $P - U_p$ plot for a flyer striking a stationary target.	24
11	Time slice from the end of an ALEGRA-HEDP simulation.	25
12	Shock position vs. time for a flyer impacting a stationary target.	26

List of Tables

1 χ^2 results comparing experimental Hugoniot data with EOS values. 10

2 Ideal simulation results compared to analytical values. 13

3 Simulated flyer impacting target results compared to analytical values. 14

Nomenclature

Term	Definition
ALEGRA	Arbitrary Lagrangian Eulerian General Research Application
EOS	Equation of State
HEDP	High Energy Density Physics
ICF	Inertial Confinement Fusion
MHD	Magnetohydrodynamics
QEOS	Quotidian Equation of State
U_P	Particle Velocity
U_s	Shock Velocity
$P - U_P$	Pressure-Particle Velocity
ρ	Density
T	Temperature
V	Specific Volume
e	Specific Energy
Energy	Specific Energy
nm	Nanometers
μm	Micrometers
ns	Nanoseconds
MBar	10^6 Bar

1 Introduction

Within the high-energy-density-physics community, SESAME [7] is the most widely referenced equation of state (EOS) implementation. When a SESAME EOS table is created, using the GRIZZLY [4] model, the PANDA [5] model, or others, several sub-models are used where each sub-model specializes in a limited region of density/temperature phase space. The outputs from these sub-models are then blended together to form a broad range EOS table. Quite often, the sub-models are adjusted to fit experimental data or theoretical approximations. Therefore, the final EOS table usually approximates the Hugoniot data to a reasonable degree (better at lower pressures). Because each table may be built to better represent different regimes of EOS phase space, there may be more than one table for each material (for example, aluminum has at least 8). As such, each table must be analyzed to ensure that it yields good results in the regime to be simulated.

This document illustrates one method of establishing confidence in the choice of an EOS for an intended simulation regime. The method is particularly helpful when SESAME tables are provided as second party information, rather than developed by the user of the table. This is the case for many of our current applications of SESAME with ALEGRA-HEDP. The steps are: comparing analytically calculated Hugoniots from the EOS table to the experimental Hugoniot data, checking thermodynamic consistency, and using impedance matching to simulate realistic hydrodynamic processes or to match with a known analytic solution. Once these steps are completed and we have selected a table, we will then run ALEGRA [2, 11] in a simple 1-D hydrodynamic shock simulation and compare the pressure and particle velocity to the analytical results of the impedance matching.

2 Calculating Hugoniots

The first step to impedance matching is to calculate the Hugoniot, which is a locus of points achievable under shock conditions, generally from ambient conditions. To do this we wrote an IDL [10] routine which uses the secant-solve method to find the root (specific volume or inverse density) of Equation 2.1. [3, 12]

$$e_i - e_0 + (P_0 + P_i) * (V_i - V_0) * 0.5 = 0.0 \quad (2.1)$$

where e is specific energy, P is pressure, V is specific volume. V_0 and P_0 are the initial volume and pressure, V_i and P_i are the volume and pressure points along the Hugoniot. Since $P(\rho, T)$ and $e(\rho, T)$ are constrained by a given temperature, the dependent variable becomes density. Therefore, we can give the Hugoniot solve routine the arrays of density, temperature, pressure $P(\rho, T)$, energy $e(\rho, T)$, and a temperature grid along which to search for Hugoniot points. Figure 1 shows several of the Hugoniot curves plotted on an EOS pressure/density plot (for scale).

The experimental data [6] is obtained as U_s/U_P data that is converted to density/pressure data by

$$P = \rho_0 U_s U_P \quad (2.2)$$

and

$$\rho = \left(\frac{1}{\rho_0} \left(1 - \frac{U_P}{U_s} \right) \right)^{-1} \quad (2.3)$$

where, for aluminum,

$$\rho_0 = 2.7 \text{ g/cm}^3 \quad (2.4)$$

U_P is particle velocity, and U_s is shock velocity.

The error bars for the data in Figure 1 are calculated using methods outlined in Reference [1].

$$\begin{aligned} \delta\rho &= \sqrt{\left(\frac{\partial\rho}{\partial U_s} \right)^2 (\delta U_s)^2 + \left(\frac{\partial\rho}{\partial U_P} \right)^2 (\delta U_P)^2} \\ &= \left(\frac{\rho}{\rho_0} - 1 \right) \rho \sqrt{\left(\frac{\delta U_s}{U_s} \right)^2 + \left(\frac{\delta U_P}{U_P} \right)^2} \end{aligned} \quad (2.5)$$

Similarly,

$$\delta P = P \sqrt{\left(\frac{\delta U_s}{U_s} \right)^2 + \left(\frac{\delta U_P}{U_P} \right)^2} \quad (2.6)$$

where δU_s and δU_P are the reported errors in the data.

Once the data is converted to the same variables as our tables, we can calculate the error between each EOS table's Hugoniot and the data using a reduced χ^2 fit. [1]

$$\chi^2 = \left(\frac{P - P_{eos}}{P_{eos}} \right)^2 \frac{1}{\delta P_{\rho}^2} + \left(\frac{P - P_{eos}}{P_{eos}} \right)^2 \frac{1}{\delta P_{pressure}^2} \quad (2.7)$$

For aluminum, the results of the reduced χ^2 are :

Table 1: χ^2 Results

EOS Table	χ^2	< 6 MBar	> 6 MBar
3700	0.116	0.050	0.188
3711	0.375	0.256	0.503
3715	0.118	0.118	0.118
3719	0.137	0.138	0.137
3720	0.087	0.069	0.106
QEOS	0.140	0.148	0.132

We chose the aluminum EOS tables most commonly used for a wide variety of simulations and computed a χ^2 for each of them. Table 1 lists those results. From the χ^2 comparison, we would choose Table 3720 for shock physics simulations in this regime, and for the remainder of this document, we will use aluminum Table 3720. For completeness, the data seems to deviate from the analytical curves at about 6 Mbar, therefore, we did an independent χ^2 test both below and above this pressure. In both cases, Table 3720 was clearly the best choice.

3 Thermodynamic Consistency

Next, because many EOS tables are spliced together from several models that are accurate within a limited regime, we must check the thermodynamic consistency of the entire blended EOS table. Figure 2 plots isothermal representations of the pressure and energy tables.

In most cases the pressure is held to be absolute and the energy is relative. Using Equation 3.8 [9],

$$T \left. \frac{\partial P}{\partial T} \right|_V - P - \left. \frac{\partial e}{\partial V} \right|_T = 0 \quad (3.8)$$

where T is temperature, P is pressure, e is specific energy, and V is specific volume, we can check for any significant errors in the table creation. In this case

$$Error = \frac{T \frac{\partial P}{\partial T} - P - \frac{\partial e}{\partial V}}{\frac{\partial e}{\partial V}} \quad (3.9)$$

However, because we have discrete data points, we cannot simply take the derivative of a function, but must take into account the slope differences on either side of each table data point. A simple way to do this is to use

$$\frac{\partial P}{\partial T} = \frac{1}{2} \left(\frac{P_i - P_{i-1}}{T_i - T_{i-1}} + \frac{P_{i+1} - P_i}{T_{i+1} - T_i} \right) \quad (3.10)$$

and similarly

$$\frac{\partial e}{\partial V} = \frac{1}{2} \left(\frac{e_j - e_{j-1}}{V_j - V_{j-1}} + \frac{e_{j+1} - e_j}{V_{j+1} - V_j} \right) \quad (3.11)$$

This differencing scheme will introduce some error ($\sim 1\%$ for a finely gridded table), but we are only looking for major problems. If two tables are similar in χ^2 and both cover the pressure/energy regime desired, then a more quantitative consistency analysis would be done. For Table 3720, there is some inconsistency in the regime just over the vapor dome (Figure 3). If we expect our material to pass through this area, we would need to quantify this error, perhaps by re-solving the energy table and re-running the simulation.

Table aluminum 3719 (Figure 4) has Maxwell constructions. Maxwell constructions replace the Van der Waals loop pressure isotherms in the vapor dome area of the pressure table with pressure isotherms that satisfy $\frac{\partial P}{\partial p} = 0$. Quite often, splicing in the Maxwell constructions when creating EOS tables leads to worse thermodynamic consistency around the edges of the vapor dome.

Aluminum 3719 does not follow the Hugoniot as well as aluminum 3720, but, from experience, we know that wire initiation problems require Maxwell constructions, therefore, we may be required to use Table 3719 anyway. However, if the simulation is going to compress and then release significantly above the vapor dome, Table 3720 would be the better table. As a check for the methods used to calculate consistency, we used QEOS [8] to generate an EOS table and then applied our consistency methods to that table. QEOS is an analytic EOS code that produces thermodynamically consistent pressure and energy results. We calculated the error using this approach where we were sure QEOS is consistent, and this error was $\sim 1\%$. We then subtracted this error from the quantified thermodynamic consistency error in Figures 3, 4, and 5 as a measure of bias in our numerical approximation of the error.

We have shown that one table is thermodynamically more consistent than another, but we do not know what effect inconsistent tables will have on any given simulation. Possible issues of an inconsistent table are overly rapid material expansion, overly slow expansion, and incorrect material heating. To examine these issues, we ran a series of isentropic release simulations and modified the pressure returned from QEOS by a constant when in a particular regime of the EOS.

We created a finely gridded table (100 points per decade) from QEOS. We then used this table to calculate a Hugoniot starting from room temperature solid. At each point along the Hugoniot, we calculated the release isentrope and continued until we found a starting density/temperature (7.156 g/cm³ and 62000 K) that released just above the vapor dome. From this starting point, the material was allowed to release as a Lagrangian free gas expansion simulation. However, for all material temperatures, if the density was between 0.5 g/cm³ and 4 g/cm³, the pressure returned from QEOS was multiplied by a constant ranging between 0.9 and 1.8.

In examining the results, we assumed the simulation without any multiplier was correct and calculated the error of the other simulations as

$$Error(\%) = \frac{Q1 - Qc}{Q1} * 100 \quad (3.12)$$

where $Q1$ is the simulation with no pressure multiplier and Qc is with a constant multiplier. Figure 6 shows the error at a time slice during the release. The thermodynamic consistency error for the baseline simulation never gets above 1%, and this error might be attributed to the fact that QEOS calculates all of the needed values ($\frac{\partial P}{\partial T}$, P etc.) internally except $\frac{\partial e}{\partial V}$ which we calculated using

$$\frac{\partial e}{\partial V} = \frac{e_V - e_{V*1.0001}}{V - V*1.0001} \quad (3.13)$$

It was found that 1.0001 to 1.00001 made very little difference in the reported thermodynamic consistency error, but much smaller caused small-divisor issues and much larger caused differencing inaccuracies.

The resulting figure shows that a 100% error in the thermodynamic consistency gives an initial simulation difference of between 20% and 40%, but that the error is not guaranteed to be constant as can be seen by comparing the error trend of the density or velocity with respect to temperature. Once the simulation has gone into an inconsistent area of the EOS, it may be dominated by that induced error for the remainder of the simulation.

An item of future work is the case where a table is locally consistent, but global inconsistent. This can occur when several tables are blended together.

4 Impedance Matching

Once the preferred table is selected, we can match the aluminum shock impedance analytically. To do this, we impact one aluminum plate on another aluminum plate of equal but opposite velocity. We chose an impact velocity of 10⁴ m/s because it is a particle velocity close to one of the experimental data points. The aluminum flyers are assumed to be infinitely thick to eliminate any rarefaction issues. For

convenience, the two plates are of the same material and equal but opposite velocities. This causes the particle velocity of both plates behind the shock to be zero because of the configuration symmetry [3]. Therefore, we set the initial velocities to $\pm 10^4$ m/s, toward each other. We then solve Equation 4.14 [3]

$$U_{particle} = U_{flyer} - \sqrt{\frac{P_{Hugoniot} - P_{initial}}{\rho_{initial}}} \sqrt{1 - \frac{\rho_{initial}}{\rho_{Hugoniot}}} \quad (4.14)$$

for the particle velocity for each of the flyers. Because the pressure and velocity must be continuous across the boundary, we can use a secant solver to iteratively find the pressure and velocity where the Hugoniot points are equal on the $P - U_P$ curve (Figure 7). Because each $P - U_P$ pair along the Hugoniot is unique, we also have the density, temperature, and energy for that point. To check the error in the iterative solver, the number of points in each curve was increased by 100 times and no appreciable difference was seen. Next, we confirmed that the ALEGRA-HEDP code can simulate the analytical problem.

5 ALEGRA-HEDP Simulation

The ALEGRA-HEDP simulation was configured as pseudo-1D Lagrangian, meaning the mesh had only one cell in the y-direction, with appropriate symmetry boundary conditions at the cell y-boundaries. The resolution in the x-direction was 10 nm per cell and the total length of the simulation was 10 μ m. The simulation was run for 0.2 ns and was stopped before the shock hit the edge of the simulation. Therefore, no rarefaction waves or secondary shocks need be taken into account. Figure 8 displays the results at the end of the ALEGRA-HEDP simulation. The error between the simulation and the analytical model for the shock velocity are:

Table 2: Ideal Simulation Results

Property	Analytical	Simulation	Error
Density	5.942801 g/cm ³	5.942414 g/cm ³	6.52×10^{-5}
Temperature	27265.84 K	27277.36 K	4.20×10^{-4}
Pressure	494.81 MBar	494.828 MBar	3.64×10^{-5}
U_P	0.0 m/s	5.9×10^{-5} m/s	<i>Round Off</i>
U_s	18.326×10^3 m/s	18.356×10^3 m/s	1.64×10^{-3}

The analytical shock velocity is Equation 5.15 [3]

$$U_{shock} = \frac{\sqrt{\frac{P_{Hugoniot} - P_{initial}}{\rho_{Hugoniot}}}}{\sqrt{1 - \frac{\rho_{initial}}{\rho_{Hugoniot}}}} \quad (5.15)$$

relative to the particle velocity. By relative to particle velocity, we mean the shock velocity is taken in the lab frame of reference, but traveling into material that is still traveling the opposite direction at some velocity. Therefore, when the shock velocity is calculated in the lab frame, the material velocity must be taken into account. Because of ringing at the shock front in the calculation (computational error), we compare to the shock speed as position of the shock over the length of the simulation, and estimate the

velocity from the slope of the resulting line. This removed the majority of the instantaneous velocity oscillations (Figure 9).

In Figure 8, there are sharp spikes at the interface between materials after impact. Currently we are assuming these are due to artificial viscosity errors. These artifacts appear in both Lagrangian and Eulerian simulations.

6 Comparing ALEGRA-HEDP with Experimental Data

ALEGRA-HEDP generated shock data has been shown to match the analytical EOS data. Now we can compare to experimental data. First, we set up the simulation to more accurately represent the experiment by impacting one flyer at an initial velocity on a stationary target plate. Figure 10 shows the expected values of shock velocity, particle velocity, and pressure based on the EOS model. Figure 11 is a time slice from the ALEGRA-HEDP simulation. The errors between the simulation and the analytical model are

Table 3: Flyer Impacting Target Results

Property	Analytical	Simulation	Error
Density	6.198652 g/cm ³	6.199115 g/cm ³	7.47×10^{-5}
Temperature	32719.83 K	32704.76 K	4.60×10^{-4}
Pressure	578.83 MBar	578.788 MBar	7.26×10^{-5}
U_p	11,000 m/s	10999.94 m/s	5.42×10^{-6}
U_s	19.489×10^3 m/s	19.496×10^3 m/s	3.60×10^{-4}

The experimental data point we are focusing on is particle velocity $11 \times 10^3 \pm 110$ m/s and shock velocity $19.4 \times 10^3 \pm 400$ m/s. We set up the simulation with the initial block velocity at 22×10^3 m/s which gives the target a particle velocity of 10999.94 m/s; its shock velocity is 19.496×10^3 m/s, which is within the error bars of the experimental data.

7 Conclusion

We have compared analytical Hugoniot points to Hugoniot points calculated from experimental data. We then chose the table that best represented that data. Next, we checked to determine if that table was thermodynamically consistent. Unfortunately, we do not currently have a test to quantify the effects of an inconsistent table, but it is assumed that material expansion will be too slow or too fast, and material heating could be incorrect. Finally, we calculated the analytical $P - U_p$ values for a flyer impacting a flyer and a flyer impacting a stationary target, and compared ALEGRA-HEDP code to those values. This demonstrated that ALEGRA-HEDP can simulate the analytical model to less than the error bars on the experimental data. As such, for simulations in this regime, ALEGRA-HEDP's evaluation of the EOS table is good to within the error bars of the experimental data.

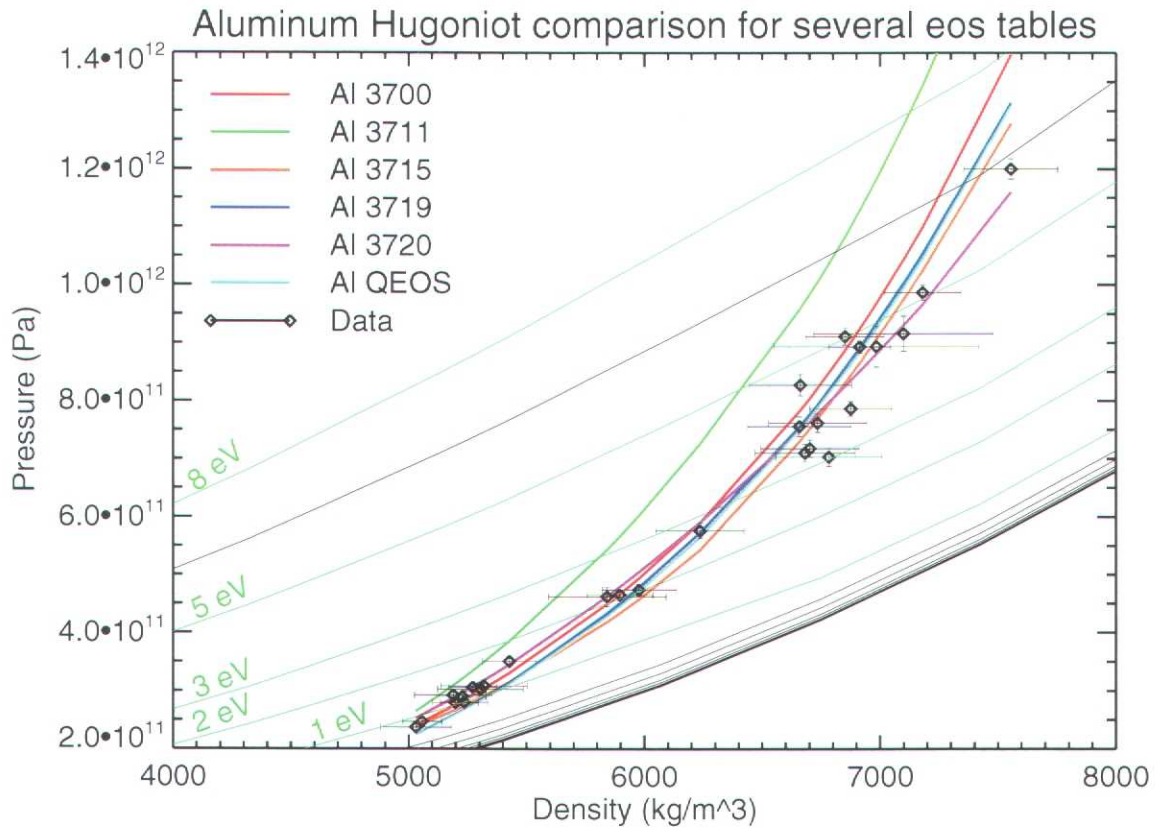


Figure 1: Hugoniot points for 6 EOS tables and experimental data on a pressure/density plot. The background lines are pressure isotherms from aluminum Table 3720. The data points are $U_s - U_p$ data that have been converted to pressure/density points. The error bars are errors in $U_s - U_p$ that have also been converted. The EOS tables plotted are those most commonly used for a wide variety of simulations.

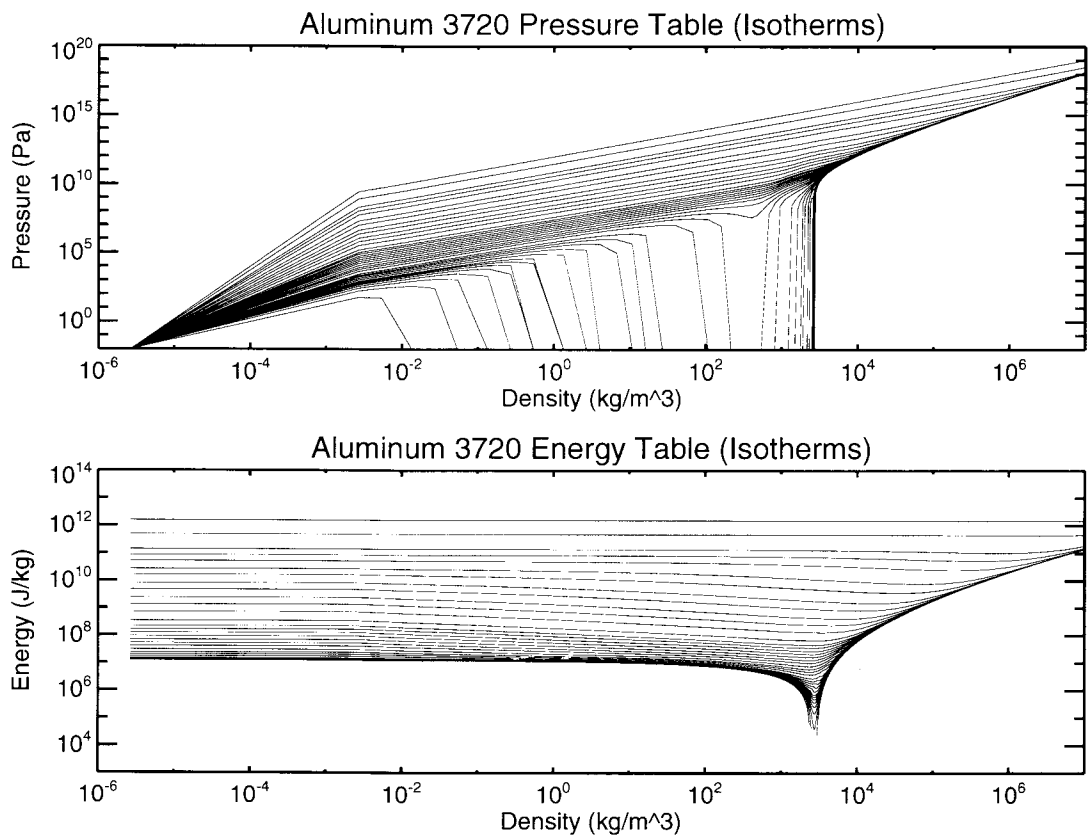


Figure 2: Aluminum 3720 EOS Tables: Pressure (Upper), Energy (Lower). These figures plot the isotherms for pressure and energy. The pressure is negative where the pressure isotherms extend off the bottom of the graph.

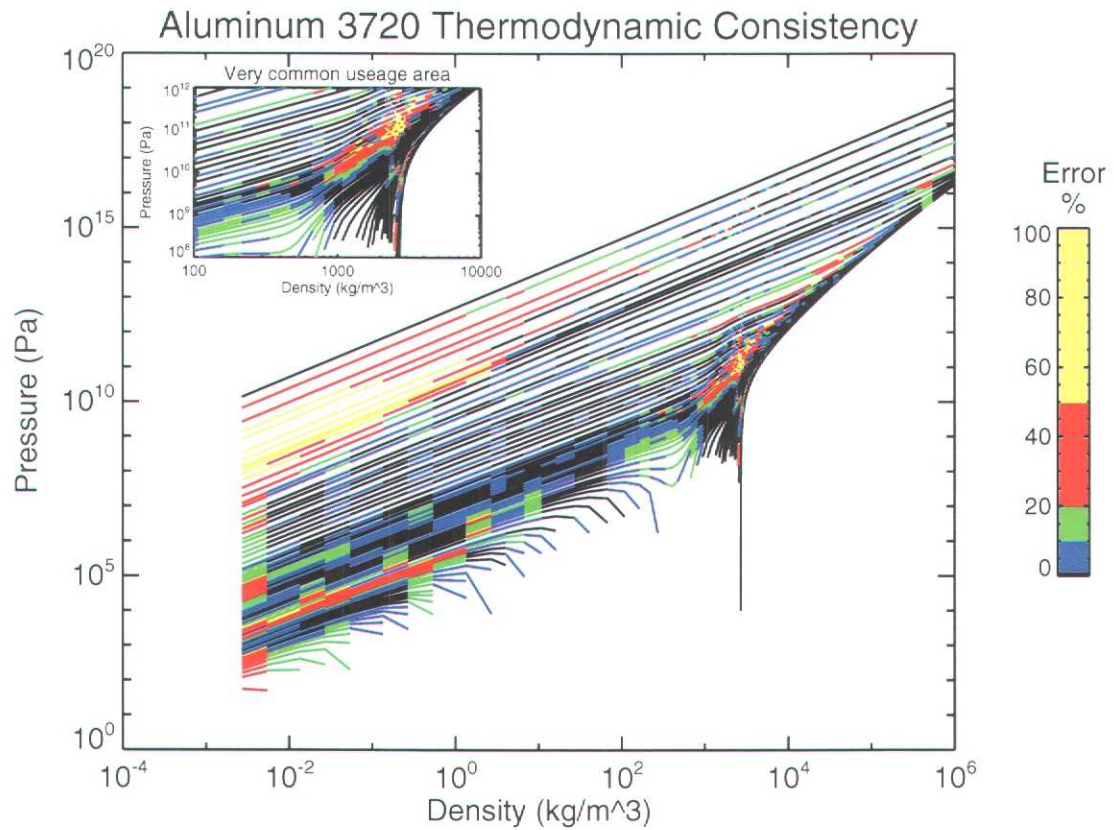


Figure 3: Error in thermodynamic consistency for aluminum Table 3720. The color scale indicates the % error in thermodynamic consistency. For simplicity, all errors above 50% are given the same color. The breaks in the pressure isotherms indicate that $P < 0$. The inlay is a regime in EOS phase space just above the vapor dome that many simulations use. (Figure should be viewed in color)

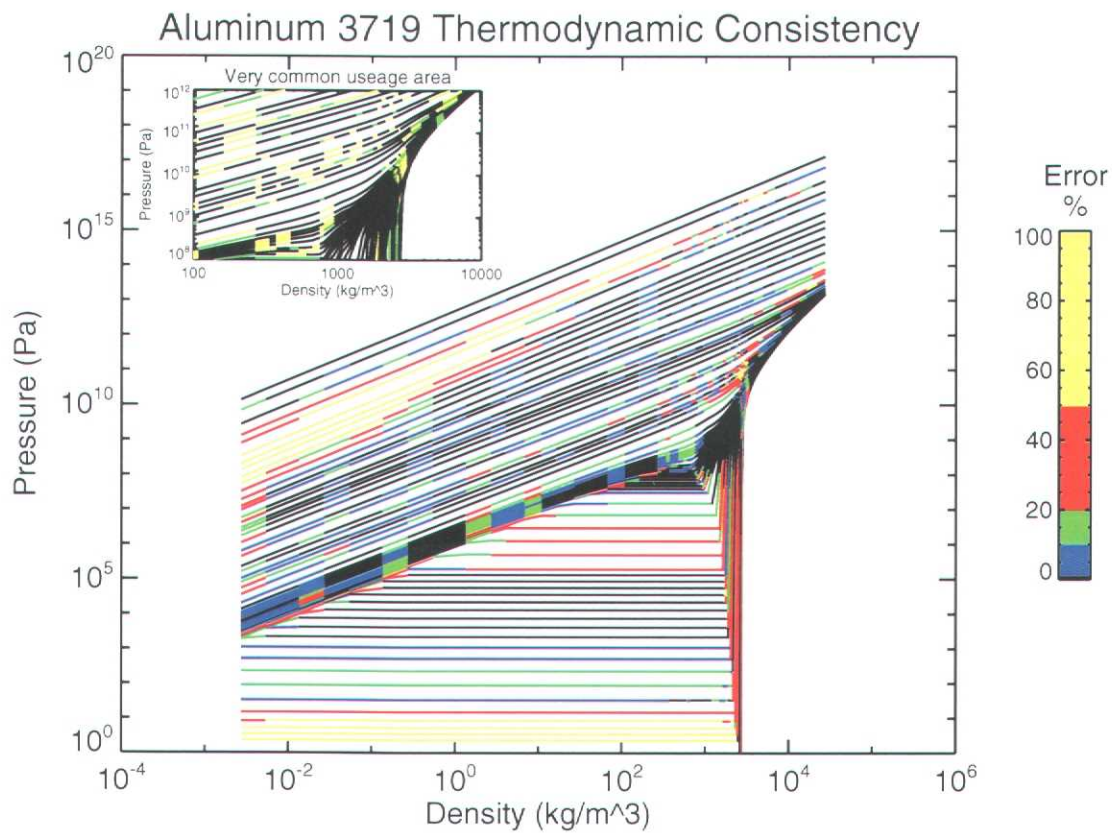


Figure 4: Error in thermodynamic consistency for aluminum Table 3719. The color scale indicates the % error in thermodynamic consistency. For simplicity, all errors above 50% are given the same color. The inlay is a regime in EOS phase space just above the vapor dome that many simulations use. (Figure should be viewed in color)

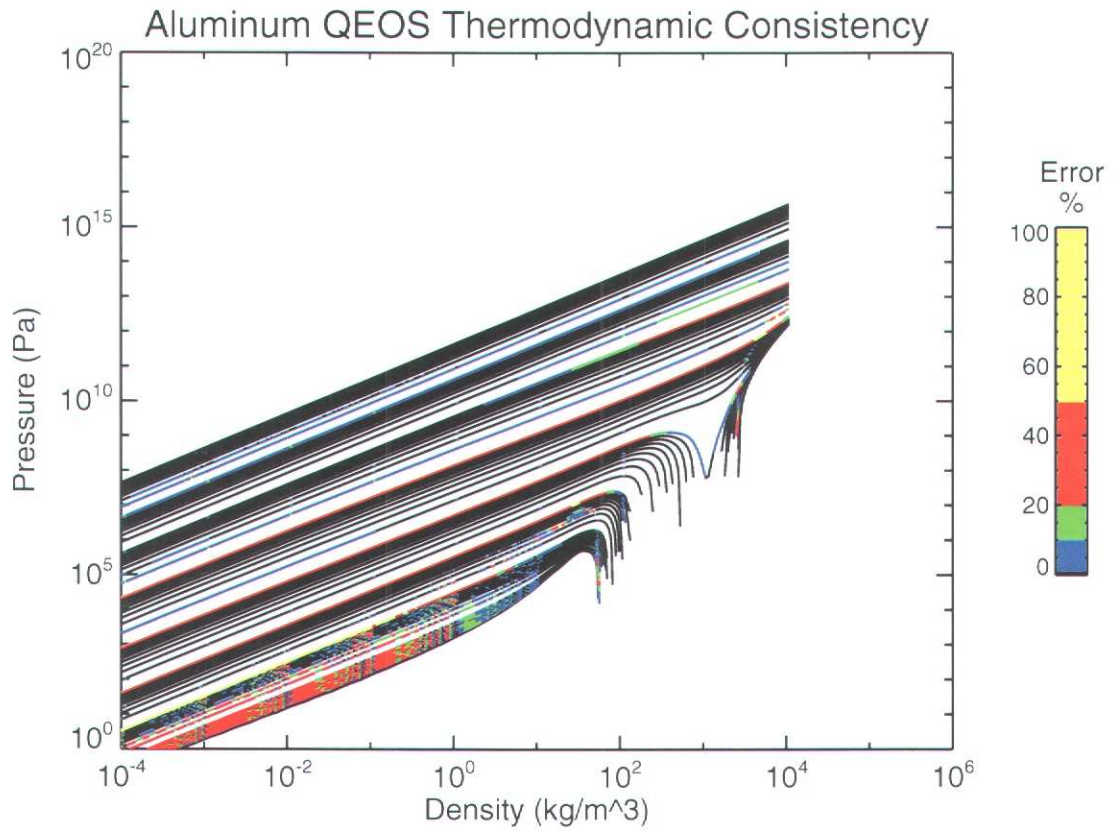


Figure 5: Error in thermodynamic consistency for aluminum QEOS. The color scale indicates the % error in thermodynamic consistency. For simplicity, all errors above 50% are given the same color. The line segments indicate $P < 0$. (Figure should be viewed in color)

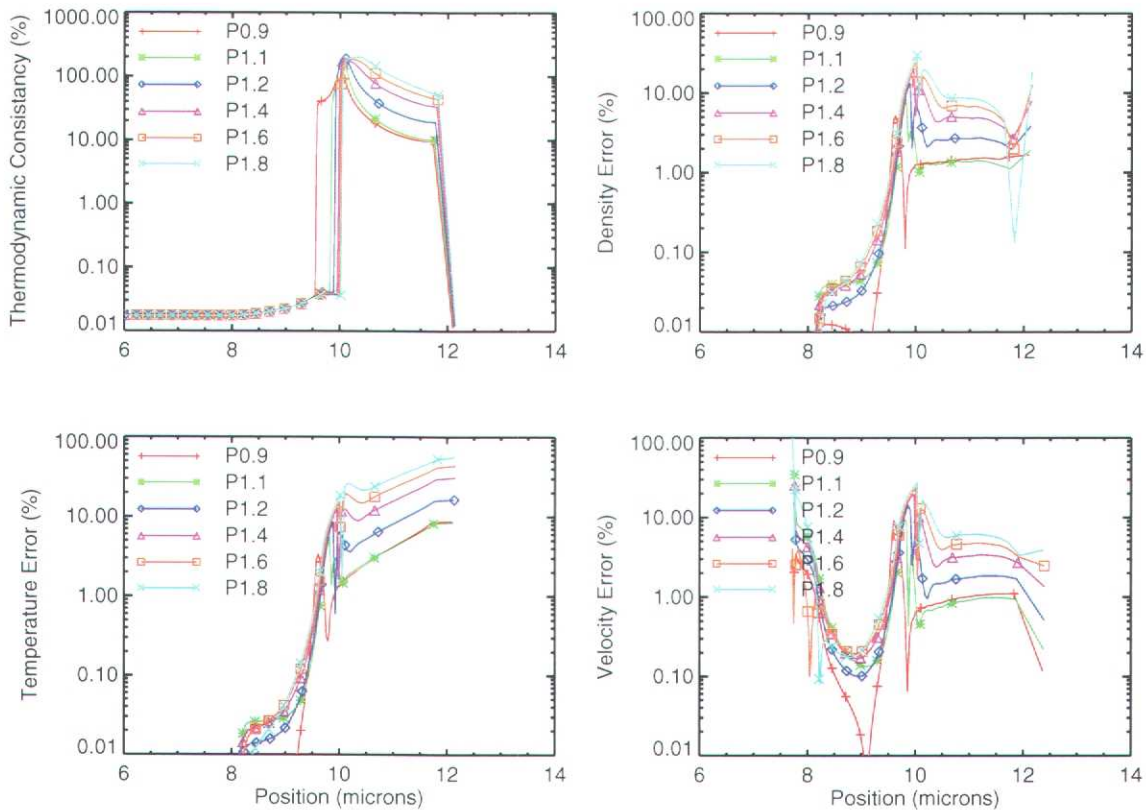


Figure 6: From a starting point of 7.156 g/cm^3 and 62000 K , a material was allowed to expand isentropically. In each simulation, as it expanded and the density decreased to between 4 g/cm^3 and 0.5 g/cm^3 , the pressure was multiplied by a constant ranging from 0.9 to 1.8. The error shown is relative to the multiplier=1.0 simulation. This figure shows the thermodynamic consistency error, density error, temperature error and velocity error for each multiplier. P0.9 signifies the pressure was multiplied by 0.9. (Figure should be viewed in color)

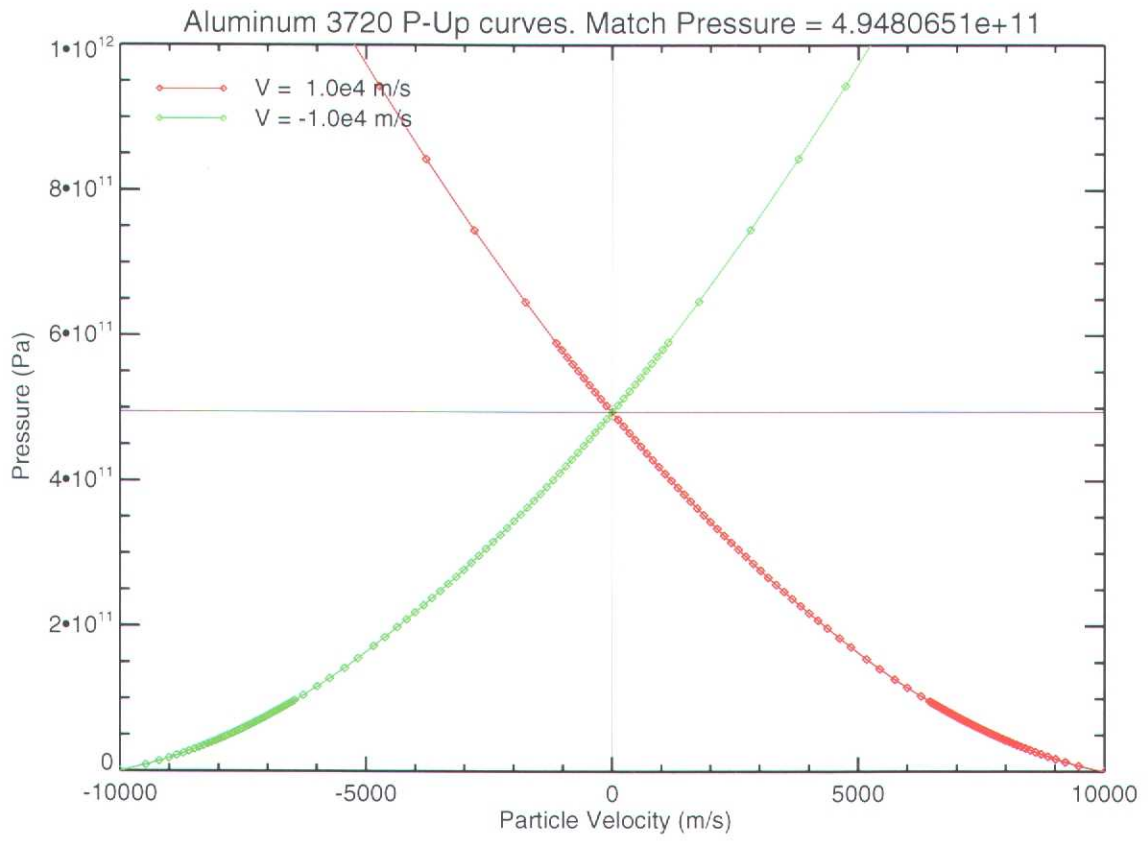


Figure 7: Impedance matching on a $P - U_p$ plot. Two flyers are launched at each other at equal and opposite velocities (10^4 m/s). Their Hugoniot curves can be mapped to pressure/particle velocity curves. Pressure and particle velocities must be continuous across an interface for two similar materials, so the curves should have a unique intersection point. This point gives the final pressure to which the material will be shocked, and the final particle velocity behind the shock.

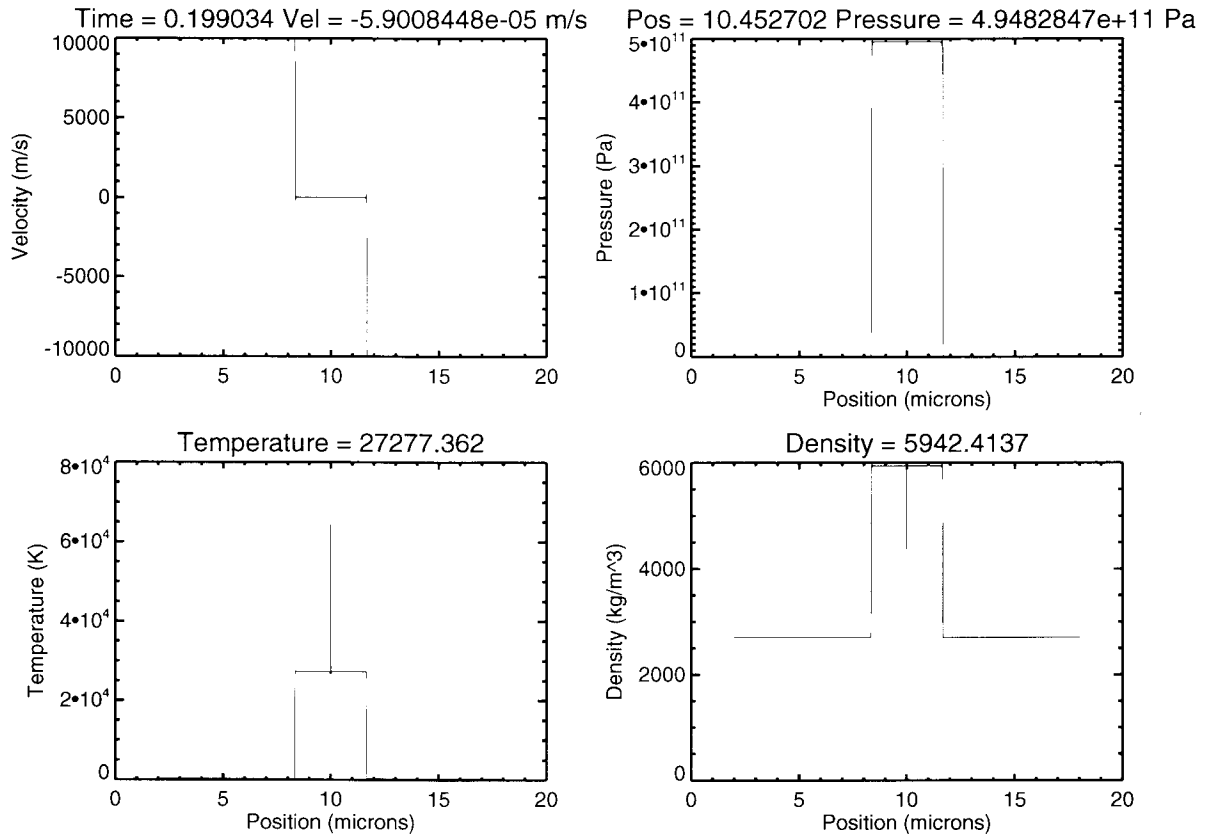


Figure 8: Time slice from the end of an ALEGRA-HEDP simulation. In this simulation two aluminum flyers were impacted with equal and opposite velocity. The sharp gradients are the interface between the shocked and unshocked material. The sharp spikes in the center of the density and temperature plots are located at the boundary between the two flyers. These high-temperature/low-density artifacts occurs regardless of the artificial viscosity. These spikes are common to most Lagrangian and Eulerian simulation codes.

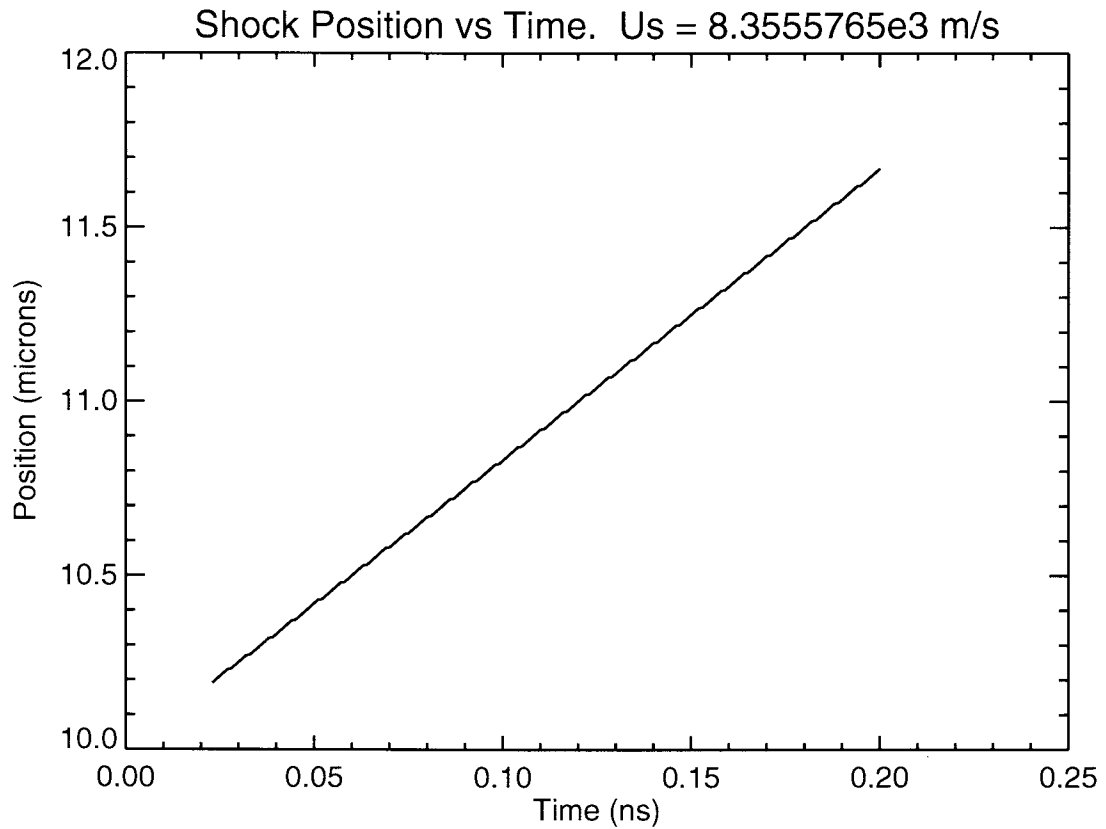


Figure 9: Shock position vs. time. Two flyers of the same material and equal but opposite velocity are impacted on each other. The shock passing through them will cause a pressure and density discontinuity. This plot tracks the position of the discontinuity as a function of time. The shock velocity is then taken as the slope of the plot. Shocks create oscillations in the EOS variables at the shock edge, so taking the position from one time step to the next could give erroneous results. The shock velocity is listed as $\sim 18 \times 10^4$ m/s because it is traveling into material that is still going the opposite direction at 10^4 m/s.

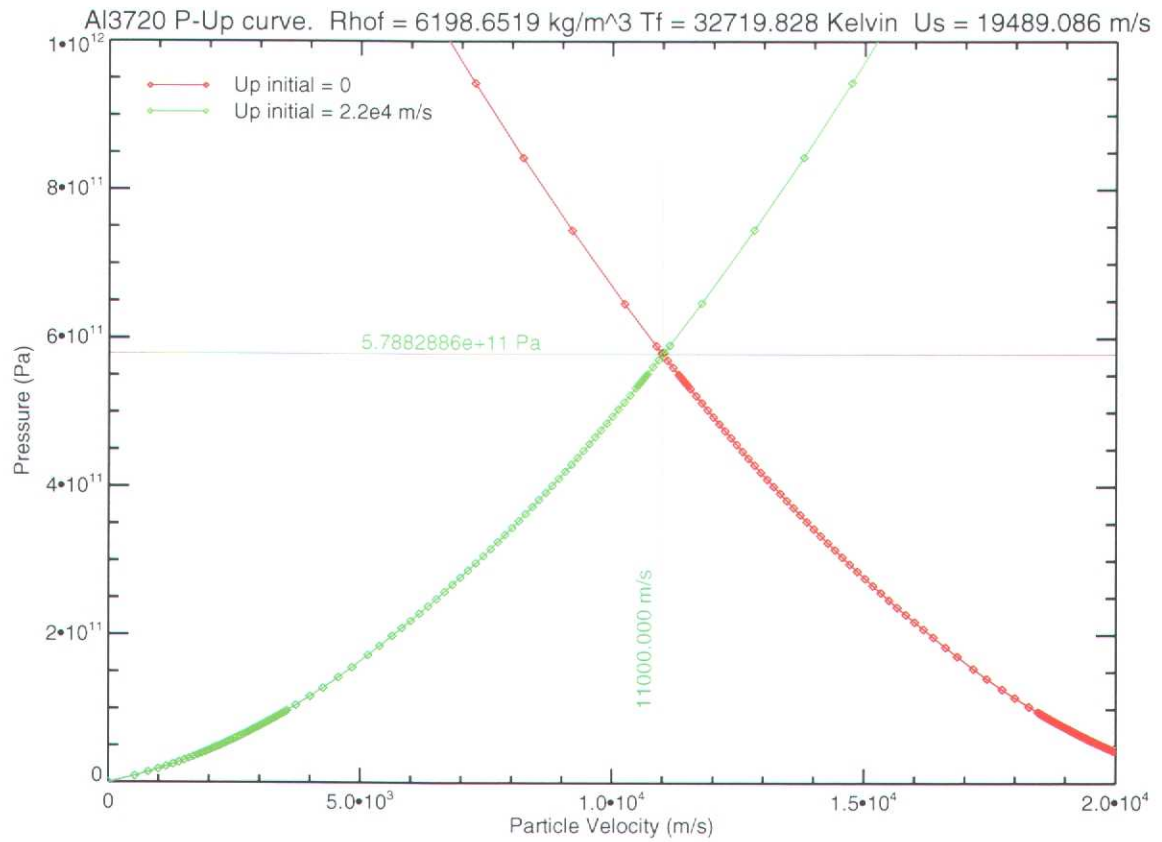


Figure 10: Impedance matching on a $P - U_p$ plot. One flyer is launched at stationary target at $22 \times 10^4 \text{ m/s}$. Note the intersection velocity is half the initial velocity.

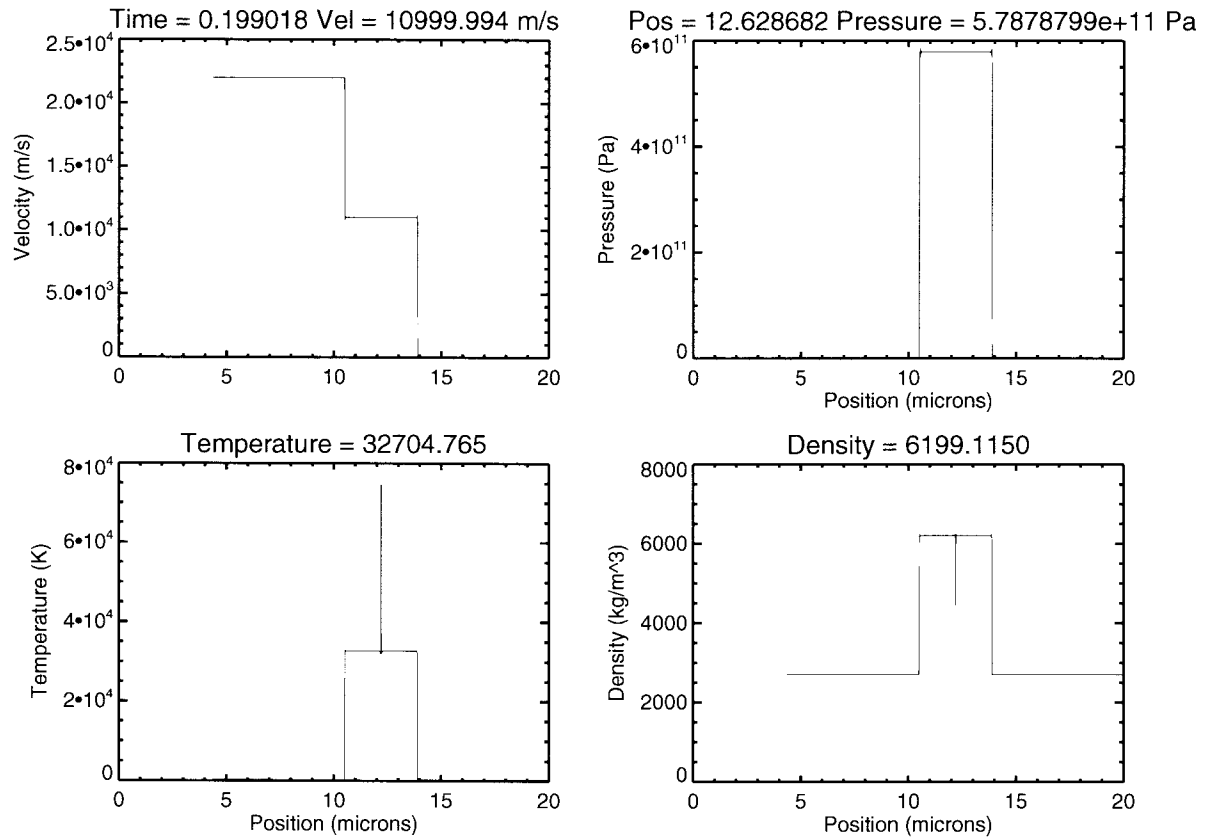


Figure 11: Time slice from the end of an ALEGRA-HEDP simulation. Note the offset from the center (10 μm). The material is traveling to the right at half the velocity of the original flyer.

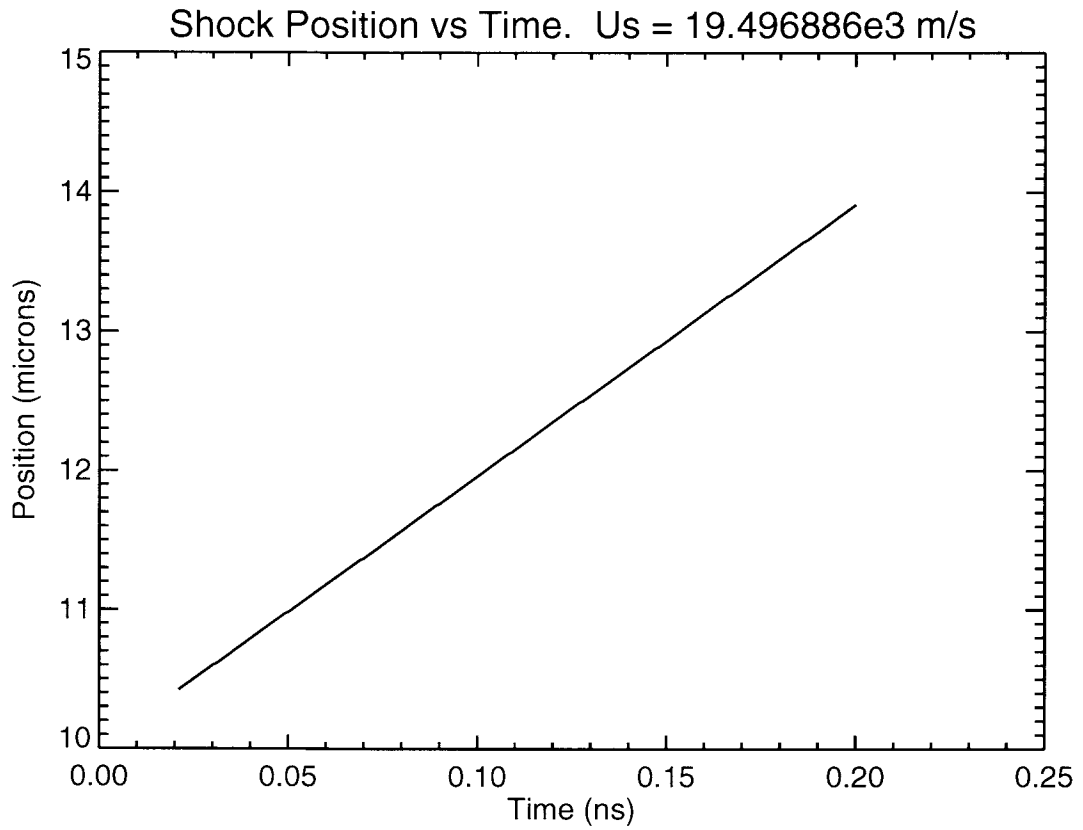


Figure 12: Shock position vs. time for a flyer impacting a stationary target. Because the shock is traveling into stationary material, the plot shows the actual shock velocity.

References

- [1] P. R. Bevington and D. K. Robinson. *Data Reduction and Error Analysis for the Physical Sciences*. McGraw-Hill, Inc, New York, 2nd edition, 1992.
- [2] S. K. Carroll et al. ALEGRA: Version 4.6. Technical report SAND2004-6541, Sandia National Laboratories, Albuquerque, NM 87185, December 2004.
- [3] D. B. Hayes. Introduction to Stress Wave Phenomena. Technical report SLA-73-0801, Sandia National Laboratories, Albuquerque, NM, 1973.
- [4] Joseph Abdalla Jr. User's Manual for GRIZZLY. Technical report LA-10244-M, Los Alamos National Laboratory, Los Alamos, NM, 1984.
- [5] G. I. Kerley. User's manual for PANDA II: A computer code for calculating equations of state. Technical report SAND88-2291, Sandia National Laboratories, Albuquerque, NM, July 1991.
- [6] M. Knudson et al. unpublished experimental $U_s - U_p$ data for aluminum. 2005.
- [7] S. P. Lyon and J. D. Johnson. SESAME: The Los Alamos National Laboratory equation of state database. Technical report LA-UR-92-3407, Los Alamos National Laboratory, Los Alamos, NM, 1992.
- [8] R. M. More, K. H. Warren, D. A. Young, and G. B. Zimmerman. A new quotidian equation of state (QEOS) for hot dense matter. *Physics of Fluids*, 31(10):3059–3078, October 1988.
- [9] F. Reif. *Fundamentals of Statistical and Thermal Physics*. McGraw-Hill, Inc, New York, 1965.
- [10] Research Systems, Inc. *Interactive Data Language (IDL)*. 4990 Pearl East Circle, Boulder, CO 80301, 2005.
- [11] R. M. Summers et al. Recent progress in ALEGRA development and application to ballistic impacts. *Int. J. Impact Engng.*, 20:779–788, 1997.
- [12] Y. B. Zel'dovich and Y. P. Raizer. *Physics of Shock Waves and High-Temperature Hydrodynamic Phenomena*. Dover, Mineola, NY, 2002.

DISTRIBUTION:

1 MS 0370 T. G. Trucano, 9211	1 MS 1186 T. A. Mehlhorn, 1674
1 MS 0378 S. V. Petney, 9231	1 MS 1186 K. Peterson, 1674
1 MS 1152 S. J. Chantrenne, 1642	1 MS 1186 E. P. Yu, 1674
3 MS 1186 K. Cochrane, 1674	1 MS 1153 L. C. Sanchez, 5541
1 MS 1186 C. J. Garasi, 1674	
1 MS 1186 T. A. Hail, 1674	
1 MS 1186 R. W. Lemke, 1674	2 MS 0899 Technical Library, 4536
1 MS 1186 T. K. Mattsson, 1674	2 MS 9018 Central Technical Files, 8945-1